PERGAMON

Scripta Materialia 46 (2002) 299–303

Scripta MATERIALIA

www.actamat-journals.com

Improvement in the ductility of molybdenum alloys due to grain boundary segregation

M.K. Miller [a,*], E.A. Kenik [a], M.S. Mousa [a,1], K.F. Russell [a], A.J. Bryhan [b]

[a] *Microscopy and Microanalytical Sciences Group, Metals and Ceramics Division, Oak Ridge National Laboratory, PO Box 2008, Oak Ridge, TN 37831-6136, USA*

[b] *Consultant, San Jose, CA 95124 USA*

Received 20 August 2001; received in revised form 15 October 2001; accepted 26 November 2001

Abstract

An improvement in the tensile ductility from the traditional 3–20% in 6.35-mm-thick molybdenum weldments has been achieved through the addition of Zr, Al, C and B at the ppm level. Atom probe tomography has revealed segregation of Zr, B and C to and depletion of O at the grain boundaries in the base metal and the heat affected zone. Published by Elsevier Science Ltd. on behalf of Acta Materialia Inc.

Keywords: Atom probe; Molybdenum; Grain boundary; Segregation; Ductility

1. Introduction

Molybdenum alloys possess an attractive combination of physical properties including high strength at elevated temperatures, high thermal conductivity, low coefficient of thermal expansion, and excellent performance in neutron flux environments. Therefore, molybdenum alloys are potential candidates for use in high temperature environments and fusion reactors. However, the low ductility of welds (typically 3% at room temperature) has limited their applications. This low ductility has been especially apparent for welds made in thick material where triaxial constraint predominates. Bryhan has shown that controlled additions of substitutional and interstitial alloying elements can provide almost 20% elongation from gas-tungsten arc (GTA) welds in 6.35-mm-thick material [1]. Several previous studies have indicated that intergranular fracture in molybdenum alloys may be caused by contaminants weakening the grain boundaries [2–5]. In this paper, these molybdenum alloys have been characterized by atom probe tomography (APT) to determine the reason for the significant improvement in ductility.

2. Experimental

The Mo used in this investigation was vacuum arc-cast with 0.15 wt.% Zr (0.16 at.%) addition intended to getter the O (42 ppm/250 appm) and N (26 ppm/178 appm) impurities together with additions of 12 ppm C (96 appm) and 6 ppm

* Corresponding author. Tel.: +1-865-574-4719; fax: +1-865-241-3650.

E-mail address: millermk@ornl.gov (M.K. Miller).

[1] On sabbatical leave from Mu'tah University, Al-Karak, Jordan.

1359-6462/02/$ - see front matter Published by Elsevier Science Ltd. on behalf of Acta Materialia Inc.
PII: S1359-6462(01)01242-8

B (53 appm) intended to strengthen the grain boundaries. The four-pass welding process was performed on 6.35-mm-thick plate in a controlled atmosphere chamber where the O, N and H_2O vapour impurity levels were each less than 10 wppm. The welding filler metal was Mo containing 30% (18 at.%) Re. A 4.5 wt.% Ti (4.7 at.%) and 1.0% Ti (2.0 at.%) Mo-TZM alloy with 100 ppm C (800 appm), and 11 ppm O (65 appm) was used as a control.

The distributions of the alloying additions in the microstructure of the base metal and the heat affected zone (HAZ) were characterized by a combination of field ion microscopy (FIM) and APT [6]. No prior examination or pre-selection of the field ion specimens in the TEM was performed in order to eliminate any possibility of carbon contamination during specimen preparation and characterization. Field ion images were recorded with He as the imaging gas and a specimen temperature of 30–50 K. APT analyses were performed with a specimen temperature of 50 K, a pulse repetition rate of 1.5 kHz and a pulse fraction of 20% of the standing voltage.

3. Mechanical properties and fractography

Tensile tests [1] were performed at room temperature at strain rates between 8.3×10^{-3} and 12.5×10^{-6} s^{-1} in stroke control. The results are summarized in Table 1. Strain was measured over two weldment regions to measure strain localization: 25 mm centered over the weld and 8.5 mm over one HAZ. Tests were performed at a standard strain rate of 8.3×10^{-4} s^{-1} and also at faster and slower rates to determine the effect of strain rate. The maximum observed total elongation, pertinent to typical engineering use, was 19.5%. Even at 8.3×10^{-3} s^{-1}, useful ductility (>10%) was apparent. The ductility of these welds is apparent by the reduction in cross-section that is visible in the optical micrograph shown in Fig. 1a and b.

Table 1
Room temperature tensile test results for GTA-welded molybdenum alloy [1]

Strain rate in 25 mm, s^{-1}	Range of elongation in gauge length (%)		Yield stress (MPa)	Ultimate tensile stress (MPa)
	25 (mm)	8.4 (mm)		
8.3×10^{-3}	10.0–12.6	7.9–11.6	537	583
8.3×10^{-4}	19.5	>15.0[a]	481	544
1.25×10^{-6}	22.6	>15.0[a]	267	457

[a] 15.0% maximum measurement with the extensometer.

Fracture was found to occur in the HAZ, as shown in optical micrographs in Fig. 1 and in the scanning electron micrograph in Fig. 2a. Some porosity was observed in the weld region, particularly close to the edge of the weld next to the HAZ. The fracture mode was transgranular cleavage, as evident in Figs. 1 and 2. This observation is in contrast to the intergranular fracture typical of welds in commercial grade molybdenum

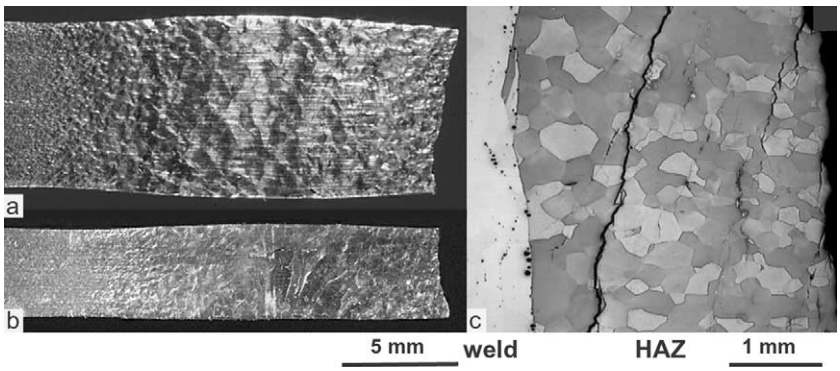

Fig. 1. Optical micrograph of a fractured tensile specimen (a) top view and (b) side view. Note the reduction in area in the base metal and HAZ. (c) Optical micrographs of cracks in the HAZ and some porosity in the weld region.

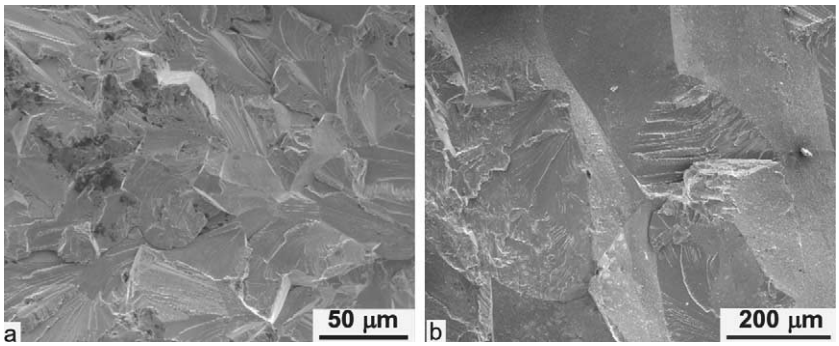

Fig. 2. Secondary electron micrographs of the fracture surface of (a) the molybdenum tensile specimen showing the transgranular mode of failure and (b) a Mo-TZM weld showing an intergranular mode of failure.

alloys, as shown in Fig. 2b for a weld in a Mo-TZM alloy fabricated with similar welding parameters, and indicates that the grain boundaries are not preferentially embrittled. This change of fracture mode suggests that the Zr, C and B alloying additions increased the grain boundary fracture stress above the yield stress.

4. Microstructural characterization

Extensive field evaporation studies of the matrix revealed no intragranular precipitates. The matrix compositions were measured in the three-dimensional atom probe and were found to be consistent with the alloy composition [7]. These matrix measurements together with the extensive field evaporation studies of the matrix indicate that no significant loss of the solute additions occurred to precipitation of phases such as oxides, carbides or borides.

Field ion micrographs of grain boundaries in the base metal and the HAZ, Fig. 3, exhibit the typical zone contrast [6] exhibited by Mo alloys and bright spot decoration [6] at the grain boundaries indicative of solute segregation. Comparison of the predicted low temperature evaporation field of Mo (41 $V\,nm^{-1}$) with the other solutes suggests that the bright spots (i.e., atoms that are more resistant to field evaporation) are B (64 $V\,nm^{-1}$) or C (103 $V\,nm^{-1}$) atoms rather than Zr (28 $V\,nm^{-1}$) atoms [8]. The level of segregation appears to be significantly higher in the HAZ than in the base metal.

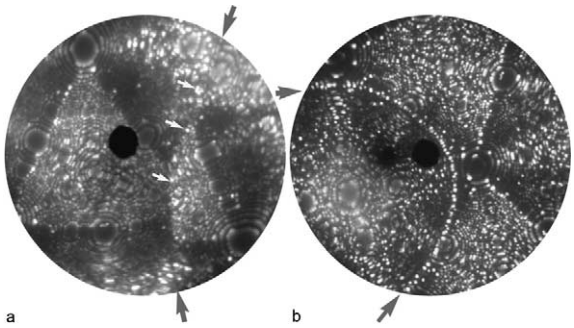

Fig. 3. Field ion micrographs of grain boundaries in (a) the base metal and (b) the HAZ. Solute decoration is significantly higher at both grain boundaries in the HAZ.

Several bright spots can be seen along the grain boundary of the base metal as indicated by arrows, whereas the grain boundary in the HAZ is continuously decorated with bright spots.

The identity of the solute species responsible for these bright spots was determined by APT [6]. Atom maps of regions of specimens that contained grain boundaries in the base metal and the HAZ are shown in Fig. 4. In these atom maps, each sphere represents the position of an atom in the volume of analysis. The molybdenum atoms have been omitted for clarity. It is evident that significant segregation of zirconium, carbon and boron to the grain boundary has occurred in the base metal. In addition, no evidence of oxygen segregation to the grain boundary was observed in the base metal. The boron segregation was found to be significantly more prevalent in the HAZ.

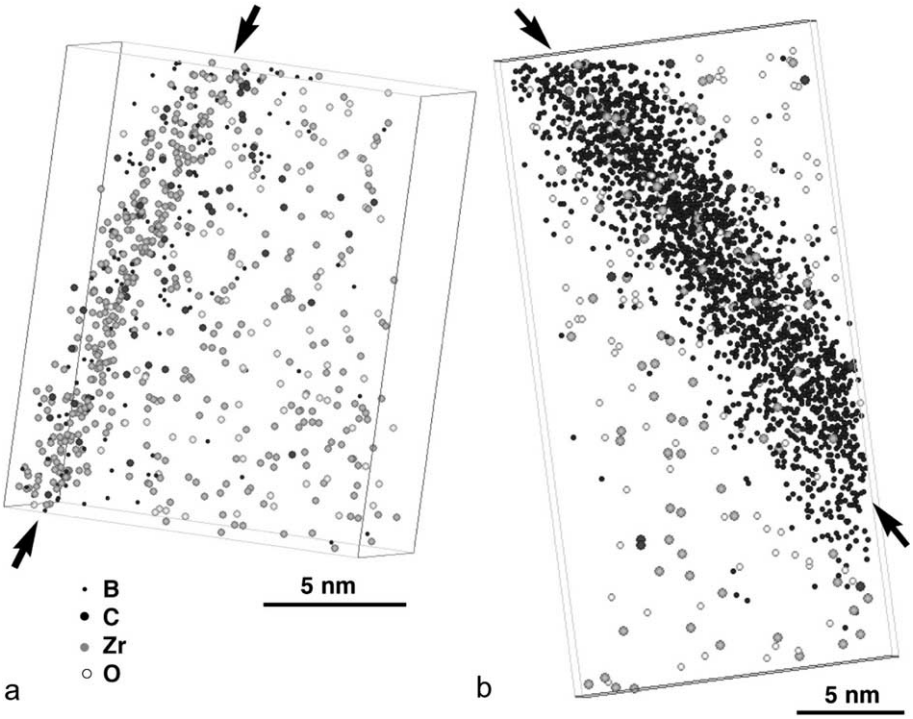

Fig. 4. Atom maps of grain boundaries in (a) the base metal and (b) the HAZ. The Mo atoms have been omitted for clarity. Each sphere represents a single atom.

The Gibbsian interfacial excesses of the solutes at these grain boundaries were determined by selected volume analyses of the grain boundary and matrix regions [6]. The results are given in Table 2. The boron excess at the grain boundary in the HAZ was two orders of magnitude higher than in the base metal, whereas the zirconium and carbon excesses in the HAZ were enriched but to a substantially lower level than in the base metal. The oxygen level at the grain boundary in the HAZ was found to be slightly enriched compared to the matrix whereas in the base metal, the oxygen level at the grain boundary was significantly reduced. A previous imaging atom probe study of a grain boundary in molybdenum revealed significant enrichment of oxygen [9]. These results suggest that the boron and zirconium additions inhibit oxygen segregation to the grain boundary in the base metal. In addition, boron segregation to the grain boundary in the HAZ minimizes or inhibits oxygen segregation to the grain boundary during the extensive grain growth that is associated with the welding process and may also reduce the amount of grain growth.

Table 2
Gibbsian interface excesses of solute at the grain boundary in the base metal and HAZ

Element	Gibbsian interfacial excess (atoms m^{-2})	
	Base metal	Heat affected zone
Zirconium	$7.6 \pm 0.6 \times 10^{17}$	$1.4 \pm 0.4 \times 10^{17}$
Carbon	$1.1 \pm 0.3 \times 10^{17}$	$9.9 \pm 9.9 \times 10^{15}$
Boron	$7.3 \pm 2.7 \times 10^{16}$	$9.9 \pm 0.2 \times 10^{18}$
Oxygen	$-3.9 \pm 0.6 \times 10^{16}$	$1.1 \pm 0.4 \times 10^{17}$

Errors are based on counting statistics of the number of atoms detected.

5. Conclusions

These APT results have demonstrated that there was no significant segregation of oxygen to any of the grain boundaries characterized in this

high ductility zirconium-, boron- and carbon-doped molybdenum alloy. The oxygen segregation may be inhibited due to the presence of zirconium, carbon and boron at the grain boundary in both the base metal and the HAZ. This change in segregation behavior correlates with a change in the observed fracture mode from the intergranular failure normally observed in commercial molybdenum alloys to transgranular failure in this zirconium-, boron- and carbon-doped molybdenum alloy.

Acknowledgements

Research at the Oak Ridge National Laboratory SHaRE Collaborative Research Center was sponsored by the Division of Materials Sciences and Engineering and the Office of Fusion Energy Sciences, US Department of Energy, under contract DE-AC05-00OR22725 with UT-Battelle, LLC.

References

[1] Bryhan AJ. Joining of Molybdenum Base Metals and Factors which Influence Ductility. WRC Bulletin 312, ISSN 0043-2326, February 1986.
[2] Stephens JR, Witzke WR. J Less Common Met 1972;29: 371.
[3] Brosse JB, Fillet R, Biscondi M. Scripta Metall 1981;15: 619.
[4] Kumar A, Eyre BL. Proc R Soc London A 1980;370:431.
[5] Suzuki A, Matsui H, Kimura H. Mater Sci Eng 1981; 47:209.
[6] Miller MK. In: Atom probe tomography: analysis at the atomic level. New York: Kluwer Academic/Plenum Press; 2000. p. 1.
[7] Miller MK, Bryhan AJ. Mater Sci Eng A, in press.
[8] Tsong TT. Surf Sci 1978;70:211.
[9] Waugh AR, Southon MJ. Surf Sci 1977;68:79.